

Elimination of Germinal Center-Derived Self-Reactive B Cells Is Governed by the Location and Concentration of Self-Antigen

Tyani D. Chan,¹ Katherine Wood,¹ Jana R. Hermes,¹ Danyal Butt,¹ Christopher J. Jolly,³ Antony Basten,^{1,2} and Robert Brink^{1,2,*}

¹Immunology Research Program, Garvan Institute of Medical Research, 384 Victoria St, Darlinghurst, Sydney NSW 2010, Australia

²St. Vincent's Clinical School, University of New South Wales, Sydney NSW 2010, Australia

³Centenary Institute, The University of Sydney, Sydney NSW 2006, Australia

*Correspondence: r.brink@garvan.org.au

<http://dx.doi.org/10.1016/j.immuni.2012.07.017>

SUMMARY

Secondary diversification of the B cell repertoire by immunoglobulin gene somatic hypermutation in the germinal center (GC) is essential for providing the high-affinity antibody specificities required for long-term humoral immunity. While the risk to self-tolerance posed by inadvertent generation of self-reactive GC B cells has long been recognized, it has not previously been possible to identify such cells and study their fate. In the current study, self-reactive B cells generated *de novo* in the GC failed to survive when their target self-antigen was either expressed ubiquitously or specifically in cells proximal to the GC microenvironment. By contrast, GC B cells that recognized rare or tissue-specific self-antigens were not eliminated, and could instead undergo positive selection by cross-reactive foreign antigen and produce plasma cells secreting high-affinity autoantibodies. These findings demonstrate the incomplete nature of GC self-tolerance and may explain the frequent association of cross-reactive, organ-specific autoantibodies with postinfectious autoimmune disease.

INTRODUCTION

Diversification of T and B lymphocyte antigen receptors is fundamental to immunity. In the case of B cell antigen receptors (BCRs), clonal diversification of the antigen-combining sites occurs in two phases. The first takes place during early B cell development when unique combinations of V, (D), and J DNA segments are assembled to form the immunoglobulin (Ig) heavy and light chain variable region genes. The products of these genes combine to define the distinct antigen-binding capabilities of the BCRs expressed on each cell within the primary B cell repertoire. Depending on their BCR binding-specificity, naive B cells may recognize and be activated by structures associated with foreign cells or molecules. Collaboration with antigen-activated CD4⁺ T helper (Th) cells follows, leading to the proliferative

expansion of activated B cells followed by their differentiation into either terminally differentiated antibody-secreting plasma cells or germinal center (GC) B cells (Goodnow et al., 2010; MacLennan, 1994, 2003).

GCs are areas of intense B cell proliferation that form around the follicular dendritic cell (FDC) networks within the follicles of secondary lymphoid tissues and also contain specialized T follicular helper (Tfh) cells (Allen and Cyster, 2008; King et al., 2008). It is typically within GCs that the second phase of BCR diversification occurs via somatic hypermutation (SHM), the introduction of point mutations into the Ig heavy and light chain variable region coding exons. Rare GC B cell clones that acquire increased affinity for foreign antigen undergo positive selection, whereby they preferentially survive, proliferate, and ultimately undergo plasma cell differentiation. This process of “affinity maturation” is driven by competition between GC B cells for foreign antigen presented in immune complexes on the FDC surface and the subsequent delivery of cognate help from T_{FH} cells (Allen and Cyster, 2008; Goodnow et al., 2010; Tarlinton, 2008; Victora et al., 2010). Thus the secondary diversification of BCRs coupled with affinity maturation in GCs provides the high-affinity serum antibodies that mediate long-term humoral immunity and form the basis of most successful vaccines (Plotkin et al., 2008).

The essentially random nature of the genetic mechanisms responsible for generating antigen receptor diversity means that the production of lymphocyte clones capable of recognizing components of host tissues (i.e., self-antigens) is inevitable. Indeed, up to 75% of newly generated bone marrow B cells express BCRs that bind to self-antigens (Wardemann et al., 2003). In order to benefit from lymphocyte diversity, therefore, the immune system has evolved a parallel series of “self-tolerance” mechanisms through which the participation of self-reactive lymphocytes in destructive autoimmune responses is largely prevented. In the case of the primary B cell repertoire, the self-tolerance mechanisms responsible for eliminating, editing, or silencing self-reactive B cells have been extensively characterized (Goodnow, 1992; Nemazee, 1993; Nossal, 1994). This has been achieved largely through the application of genetically modified mouse models that have allowed BCR specificities within the primary repertoire to be directed toward a natural or transgene-encoded self-antigen. By contrast, the dynamic and complex nature of GCs has so far thwarted attempts to identify and study self-reactive B cells generated during the formation

of the secondary repertoire by SHM. This has greatly limited insights into how self-tolerance is enforced in the GC and how residual self-reactive GC B cells may contribute to autoimmunity.

The potential for B cells to acquire self-reactivity via SHM has been verified both in vitro (Casson and Manser, 1995; Diamond and Scharff, 1984) and in vivo (Olee et al., 1992; Shlomchik et al., 1990; Shlomchik et al., 1987; Tiller et al., 2007). The demonstration that somatically mutated, pathogenic autoantibodies can emerge from the GC indicates that self-tolerance within the secondary B cell repertoire is not absolute. Nevertheless, several studies suggest that self-reactive GC B cells may be eliminated following interaction with self-antigen. These include experiments in which the injection of a bolus of exogenous antigen has resulted in widespread apoptosis of antigen-specific GC B cells (Han et al., 1995; Pulendran et al., 1995; Shokat and Goodnow, 1995) and a model in which class-switched IgG2a⁺ B cells are eliminated by a transgenically encoded anti-IgG2a “superantigen” (Ait-Azzouzene et al., 2010). Evidence also exists that naive B cells that have some self-reactivity can emerge from the GC having lost self-reactivity as a result of SHM (Casson and Manser, 1995; Guay et al., 2004; Notidis et al., 2002). Although it would appear that self-reactive GC B cells may be inactivated under some circumstances, the current absence of a model with which to identify bona fide self-reactive B cells generated within the GC has made it difficult to determine how these cells are inactivated and under what circumstances this does or does not occur.

Here we have described a new experimental model that allows the precise identification and analysis of B cells acquiring self-reactivity in the GC. In particular, this model examines those GC B cells that represent the greatest autoimmune threat; that is, the self-reactive clones that acquire self-reactivity via SHM but retain the potential to undergo positive selection by foreign antigen. Selection against such self-reactive clones was found to occur but to be critically dependent on the concentration and location of self-antigen expression. Moreover, the data indicate that competition for self versus foreign antigen in the GC microenvironment is fundamental in determining the fate of self-reactive specificities generated by SHM.

RESULTS

A Model for Investigating Self-Reactive GC B Cells: HEL^{3X} and HEL^{4X} as Homologous Foreign and Self-Antigens

The first requirement for an experimental model to identify and study self-reactive GC B cells was a population of B cells that possessed a defined and well-characterized BCR specificity. In addition, a pair of homologous foreign and self antigens were required such that: (1) the foreign but not the self-antigen binds to the BCR (i.e., naive B cells are not self-reactive) and (2) somatically mutated GC B cells gaining increased affinity for the foreign-antigen also acquire cross-reactivity with the self-antigen (see Figure S1A available online).

As a basis for this model, B cells derived from the SW_{HEL} line of Ig transgenic mice were utilized. B cells from SW_{HEL} mice express BCRs with the specificity of the HyHEL10 monoclonal

antibody and thus bind to the foreign protein hen-egg lysozyme (HEL) with high affinity (Padlan et al., 1989; Phan et al., 2003). Because the VDJ exon of HyHEL10 is targeted to the endogenous Ig heavy chain locus, anti-HEL SW_{HEL} B cells undergo normal Ig class switching and SHM (Phan et al., 2006). To facilitate studies of affinity maturation using SW_{HEL} B cells, we previously developed HEL^{3X}, a recombinant form of HEL with three amino-acid substitutions in the HyHEL10 binding site (Paus et al., 2006) (Figure 1A). The binding of HEL^{3X} to HyHEL10 is of intermediate affinity ($K_a = 1.1 \times 10^7 \text{ M}^{-1}$) and is readily detectable by direct ELISA (Figure 1C). Despite its reduced affinity for the SW_{HEL} BCR, HEL^{3X} coupled to sheep red blood cells (HEL^{3X}-SRBC) elicits a strong in vivo proliferative response from donor (CD45.1 congenic) SW_{HEL} B cells upon adoptive transfer into wild-type (WT) recipient mice (Figure 1E). This response includes the formation of GCs by donor SW_{HEL} B cells in which somatically mutated, high-affinity, anti-HEL^{3X} clones accumulate due to positive selection (Phan et al., 2006). The great majority of these affinity-matured SW_{HEL} GC B cells carry a canonical Y53D substitution in the Ig heavy chain variable region, which results in a >100-fold increase in the affinity of HyHEL10 for HEL^{3X} (Phan et al., 2006).

To develop a self-antigen to use in partnership with HEL^{3X} foreign antigen, we introduced an additional amino acid substitution (K97R) into the HyHEL10 binding site of HEL^{3X}. The resulting recombinant protein was designated HEL^{4X} (Figure 1B). Although HEL^{4X} maintained a quantifiable affinity for HyHEL10 ($K_a = 2.3 \times 10^5 \text{ M}^{-1}$), the very low affinity of this interaction made it undetectable by ELISA (Figure 1C). Moreover, HEL^{4X} proved incapable of triggering a measurable in vitro response from SW_{HEL} B cells (Figures S1B–3E) and could not elicit a response from SW_{HEL} B cells in vivo when conjugated to SRBCs (Figure 1E). However, HEL^{4X} was found to bind strongly ($K_a = 2.8 \times 10^7 \text{ M}^{-1}$) to Y53D-substituted HyHEL10 (Figures 1D). Thus HEL^{4X} does not have a biologically relevant interaction with the initial SW_{HEL} BCR but does bind to the Y53D mutated form selected during the GC response of SW_{HEL} B cells to HEL^{3X}-SRBC.

Transgenic Mice Expressing Membrane-Bound HEL^{4X} as a Self-Antigen

To establish a system in which HEL^{4X} was expressed as a bona fide self-antigen, a line of mice was required that expressed HEL^{4X} from a stably integrated transgene. To this end, mice were produced carrying a cDNA encoding a membrane-bound form of HEL^{4X} (mHEL^{4X}) driven by a ubiquitously expressed promoter (UBC) and introduced as a single copy into the ROSA26 locus (Figure 2A; Figure S2). Two separate lines of mice were derived in which a polyadenylation site flanked by loxP recombination sequences was either present or absent from between the promoter and cDNA sequences (Figure 2A). In mice lacking the polyadenylation site (mHEL^{4X} Tg mice), mHEL^{4X} self-antigen was expressed in all tissues examined (Figure 2B). Flow cytometric analysis demonstrated the presence of mHEL^{4X} on all tested hematopoietic cell types from mHEL^{4X} Tg mice (Figure 2C). Immunofluorescence histology also indicated that mHEL^{4X} self-antigen was expressed throughout the spleens of these mice, including in GCs (Figure 2D).

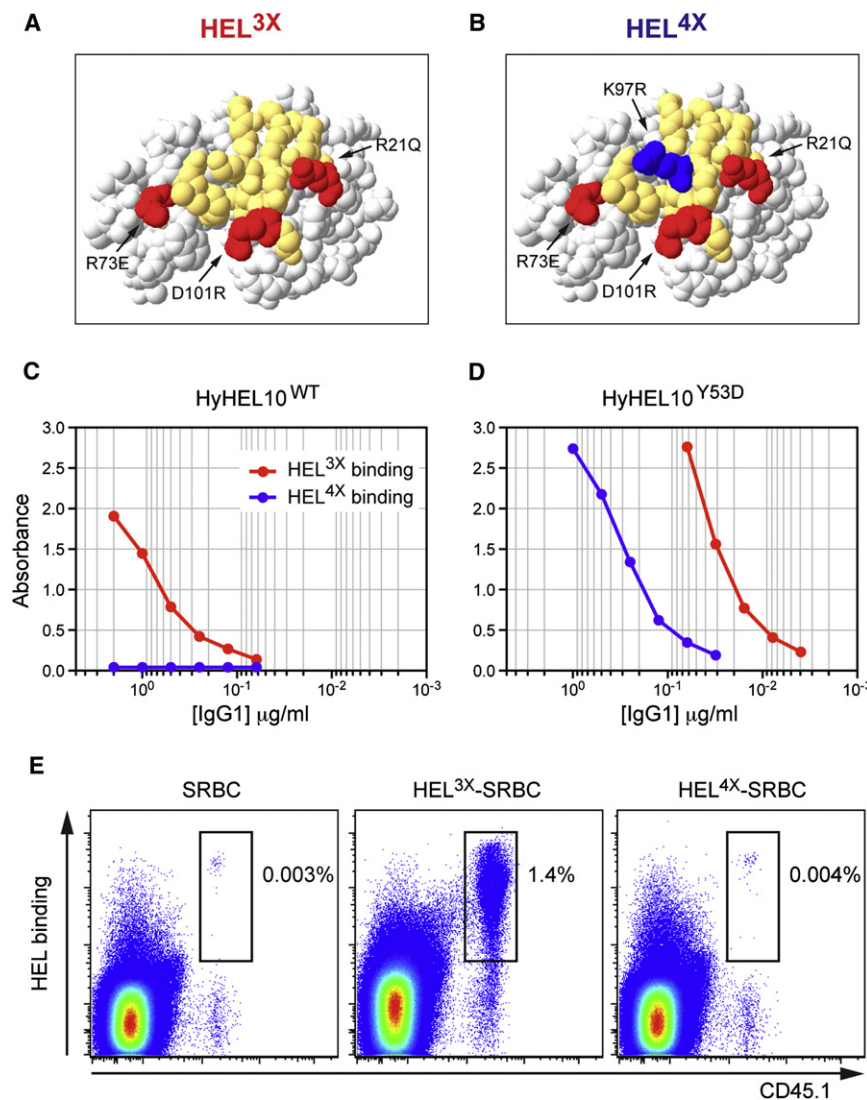


Figure 1. Production of HEL^{4X} and Demonstration of Its Binding to Y53D-Substituted but Not WT HyHEL10

(A and B) Space filling models of HEL^{3X} (A) and HEL^{4X} (B). Residues involved in HyHEL10 binding are yellow with substitutions common to HEL^{3X} and HEL^{4X} in red and the substitution unique to HEL^{4X} (K97R) in blue.

(C and D) ELISA of the binding of recombinant IgG1 mAbs HyHEL10 (C) and HyHEL10^{Y53D} (D) to HEL^{3X} (red) and HEL^{4X} (blue).

(E) Flow cytometry of spleen cells from WT (CD45.2⁺) recipient mice 5 days after injection with CD45.1 congenic SW_{HEL} B cells and the indicated SRBC conjugate. SW_{HEL} B cells express the WT form of HyHEL10 as their BCR and proliferate in response to HEL^{3X}-SRBC but not unconjugated SRBC or HEL^{4X}-SRBC. Plots are representative of three independent experiments and comprise concatenated data from two recipient mice.

was apparent in mHEL^{4X} Tg recipients (Figure 3C). In contrast to WT recipients, however, development of cross-reactivity with HEL^{4X} was absent (Figure 3D). Thus, while affinity maturation of SW_{HEL} GC B cells in response to HEL^{3X} foreign antigen could operate in mHEL^{4X} Tg recipients, HEL^{3X}-binding clones that cross-reacted with mHEL^{4X} self-antigen were apparently prevented from undergoing positive selection. Immunohistology analysis confirmed that the selection of GC phenotype B cells occurred within GC structures in spleens from both recipient genotypes (Figure S3).

To obtain a clearer picture of how mHEL^{4X} self-antigen expression was shaping the GC response to HEL^{3X}-

Ubiquitous, High Expression of Self-Antigen Prevents Positive Selection of Cross-Reactive GC B Cells

To determine the fate of GC B cells that cross-react with a ubiquitous self-antigen, donor SW_{HEL} B cells were injected into mHEL^{4X} Tg or control WT recipient mice and challenged with HEL^{3X}-SRBC foreign antigen. Under these circumstances, IgG1 is the major class switched isotype expressed by responding SW_{HEL} B cells (Chan et al., 2009). Flow cytometric analysis of donor SW_{HEL} GC B cells (CD45.1⁺, B220⁺, CD38^{low}) in WT recipients revealed that clones with increased affinity for HEL^{3X} accumulated between days 5 and 14 of the response (Figure 3A). As predicted by the binding of Y53D-substituted HyHEL10 to HEL^{4X} (Figure 1D), SW_{HEL} GC B cells undergoing affinity maturation to HEL^{3X} foreign antigen in WT recipients also developed cross-reactivity with HEL^{4X} by day 14 of their response to HEL^{3X}-SRBC (Figure 3B).

In mHEL^{4X} Tg recipient mice, the response of donor SW_{HEL} B cells to HEL^{3X}-SRBC generated normal frequencies of both IgG1⁺ and IgG1⁻ GC B cells on day 5 (Figure 3C). By day 14, affinity maturation of SW_{HEL} GC B cells to HEL^{3X} foreign antigen

SRBC, SHM analysis was performed by sequencing the Ig heavy chain variable region exon from single SW_{HEL} GC B cells isolated on days 14 and 35. The most strongly selected mutations were those resulting in the Y53D and Y58F substitutions (Figure 3E). As expected, GC B cell clones carrying the Y53D substitution dominated in WT recipients. However, Y53D⁺ clones were virtually absent from GC B cells in mHEL^{4X} Tg mice (Figure 3E, Tables S1 and S2). The Y58F substitution, by contrast, was selected in GCs from both WT and mHEL^{4X} Tg recipients. As a result, GC responses in WT recipients were dominated initially by Y53D⁺,Y58F⁻ and subsequently by Y53D⁺,Y58F⁺ clones, whereas GC responses in mHEL^{4X} Tg recipients primarily selected Y53D⁻,Y58F⁺ B cells (Figure 3F).

Analysis of recombinant HyHEL10 IgG1 antibodies carrying the Y53D and/or Y58F substitutions revealed that each bound HEL^{3X} foreign antigen with increased affinity compared to WT HyHEL10 (Figures 4A and 4B). On the other hand, binding to HEL^{4X} in ELISA was apparent for HyHEL10 molecules carrying Y53D (with or without Y58F) but not when Y58F was present alone (Figure 4B). This was consistent with the relative

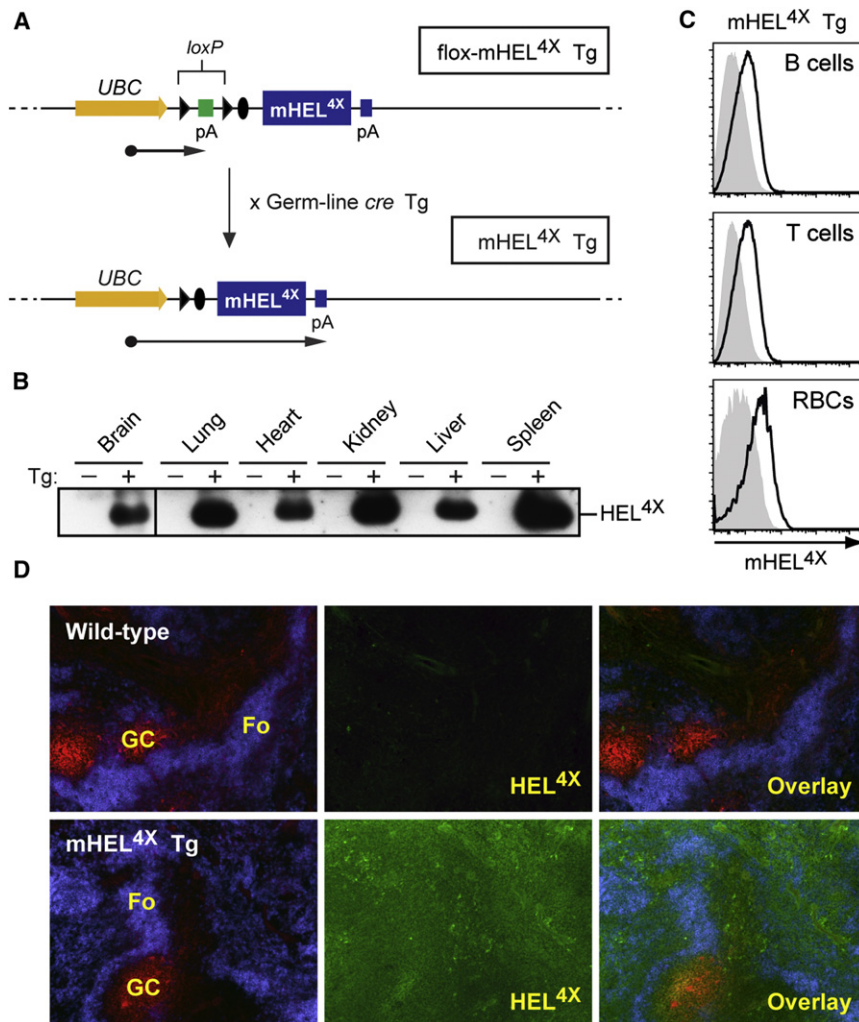


Figure 2. Construction of mHEL^{4X} Tg Mice and Analysis of mHEL^{4X} Expression

(A) Diagrammatic representation of the flox-mHEL^{4X} transgene and derivation of the mHEL^{4X} transgene with Cre. UBC, human ubiquitin C promoter; pA, polyadenylation sites; triangles, loxP sites; oval, residual FRT site (see Figure S2). (B) Immunoprecipitation and protein immunoblot analysis of mHEL^{4X} expression in tissues from WT (-) and mHEL^{4X} Tg (+) mice.

(C) Expression of mHEL^{4X} on spleen cell subpopulations from mHEL^{4X} Tg mice (open histograms) revealed by staining with HyHEL9. Grey histograms represent WT controls.

(D) Fluorescence immunohistology of spleen sections from WT (top panels) and mHEL^{4X} Tg (bottom panels) mice. B cell follicles (Fo, anti-IgD, blue), GCs (PNA, red), and mHEL^{4X} expression (anti-HEL, green) are shown. Data are representative of spleens from six individual mice of each genotype from two independent experiments.

Reduced Self-Antigen Expression Raises the Affinity Threshold of GC B Cell Self-Tolerance

To assess the impact of reduced concentrations of self-antigen expression on the development of cross-reactive GC B cells, SW_{HEL} B cells and HEL^{3X}-SRBC were injected into recipient mice expressing low but detectable amounts of mHEL^{4X} (flox-mHEL^{4X} Tg) (Figure 5A) from the same ubiquitously expressed UBC promoter utilized by mHEL^{4X} Tg mice (Figure 2A). In contrast to responses in mHEL^{4X} Tg recipients, SW_{HEL} donor GC B cells in flox-mHEL^{4X} Tg mice acquired increased affinity for HEL^{4X}

affinities for HEL^{4X} measured using Biacore analysis (Y53D⁺, Y58F⁺ $K_a = 1.1 \times 10^8 \text{ M}^{-1}$; Y53D⁺, Y58F⁻ $K_a = 2.8 \times 10^7 \text{ M}^{-1}$; Y53D⁻, Y58F⁺ $K_a = 8.9 \times 10^5 \text{ M}^{-1}$. Figure 4A; Figure S4). Serum IgG1 antibody responses to HEL^{3X}-SRBC in recipient mice, which we have shown previously to be derived exclusively from donor SW_{HEL} B cells in this experimental system (Phan et al., 2005), were as predicted by specificities detected in the GC. Thus, whereas antibodies binding HEL^{3X} foreign antigen were generated in both WT and mHEL^{4X} Tg recipients, large amounts of anti-HEL^{4X} IgG1 were only detected in WT recipients (Figure 4C). These data demonstrate that self-reactive anti-HEL^{4X} (Y53D⁺) GC B cells are effectively prevented from undergoing positive selection in mHEL^{4X} Tg mice, despite their high-affinity cross-reactivity with HEL^{3X} foreign antigen ($K_a > 3 \times 10^9 \text{ M}^{-1}$, Figure 4A). However, clones that instead acquired increased affinity for HEL^{3X} foreign antigen while avoiding high-affinity cross-reactivity with HEL^{4X} self antigen (e.g., Y53D⁻, Y58F⁺) escaped negative selection, underwent normal positive selection, and contributed to an affinity-matured antibody response against the HEL^{3X} foreign-antigen.

self-antigen, albeit not as high as that observed in WT recipients (Figure 5B). Consistent with this, day 21 SHM analysis revealed that approximately half the GC B cells present in flox-mHEL^{4X} Tg mice had undergone positive selection for the Y53D substitution (Figure 5C; Figure S5), which bestowed strong binding to HEL^{4X} ($K_a = 2.8 \times 10^7 \text{ M}^{-1}$, Figure 4A; Figure S4). However, the Y58F substitution, which increased the affinity of Y53D⁺ clones for HEL^{4X} by a further 4-fold ($K_a = 1.1 \times 10^8 \text{ M}^{-1}$, Figure 4A; Figure S4), was not strongly selected in flox-mHEL^{4X} Tg recipients and only rarely present in conjunction with Y53D (Figure 5C; Figure S5). In contrast to mHEL^{4X} Tg recipients, flox-mHEL^{4X} Tg mice contained high titers of anti-HEL^{4X} IgG1 antibodies in their serum (Figure 5D). Thus, whereas low expression of HEL^{4X} self-antigen prevented positive selection of the highest affinity self-reactive GC B cells (Y53D⁺, Y58F⁺), self-reactive Y53D⁺, Y58F⁻ GC B cells persisted in these mice and generated a clear, affinity matured, class-switched autoantibody response. These data show that competition between foreign and self-antigen, impacted upon by both their relative concentrations and affinities for the BCR, is fundamental in determining whether self-reactive GC B cells can be positively selected by

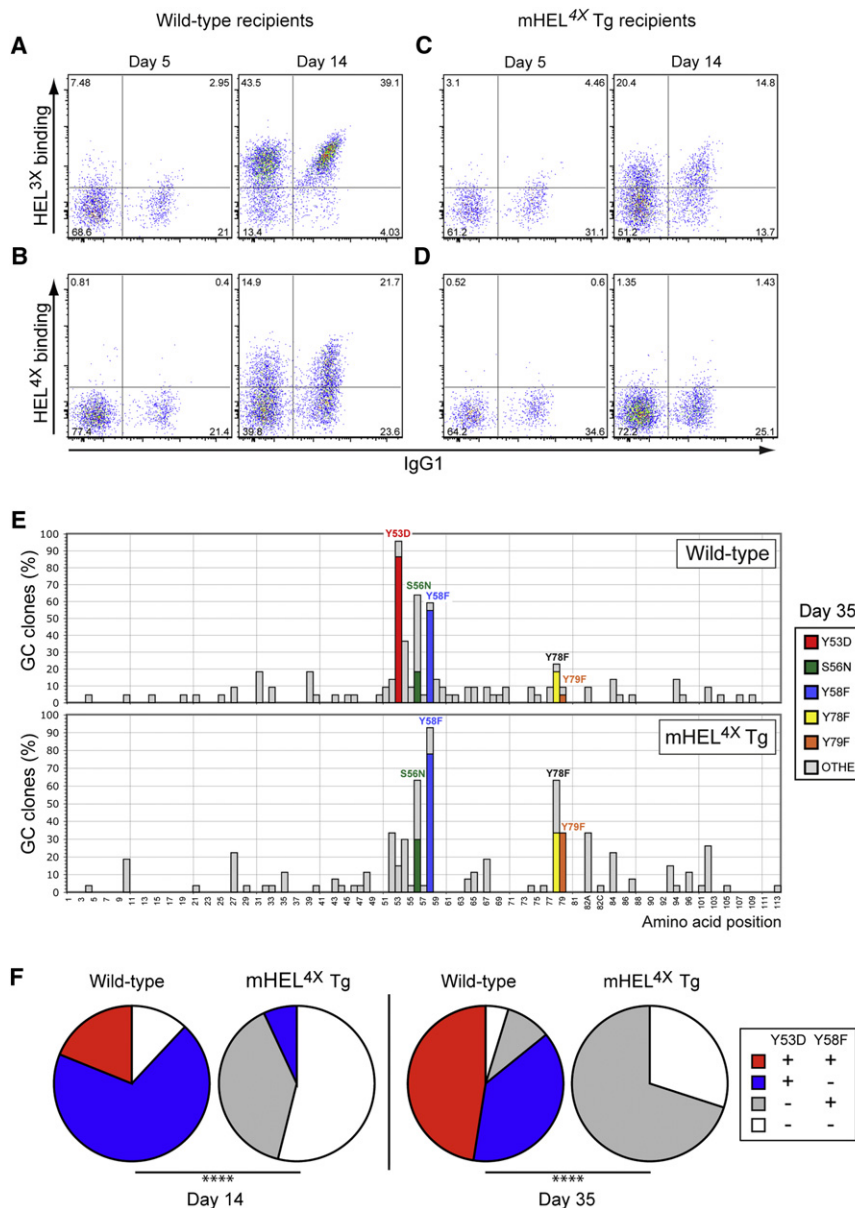


Figure 3. Failure of Self-Reactive GC B Cells to Develop in mHEL^{4X} Tg Mice

(A–D) Switching to IgG1 and HEL^{3X} versus HEL^{4X} binding capabilities of SW_{HEL} GC B cells on days 5 and 14 of responses to HEL^{3X}-SRBC. Data represent donor SW_{HEL} GC B cells (CD45.1⁺, CD45.2⁺, B220⁺, CD38^{lo}) in WT (A and B) and mHEL^{4X} Tg (C and D) recipients. Plots comprise concatenated data from three mice and representative of three independent experiments (n = 2–4 per experimental group).

(E) Single cell SHM analysis of the IgH V-region of SW_{HEL} GC B cells on day 35. Grey columns indicate the percentage of donor-derived GC B cell clones carrying substitutions at each amino acid residue. Colored bars indicate specific substitutions present in >20% of clones in WT and/or mHEL^{4X} Tg recipients on day 35.

(F) Single cell SHM analysis of SW_{HEL} GC B cells on days 14 and 35. Sectors indicate fraction of clones with the indicated combinations of Y53D and Y58F substitutions. Clones analyzed are as follows: WT recipients (d.14, n = 32; d.35, n = 22) and mHEL^{4X} Tg recipients (d.14, n = 28; d.35, n = 29). Data from each group are derived from two mice. ****p < 0.0001.

This replicated the phenotype of tolerant mHEL^{4X} Tg recipients (Figures 4 and 6E) despite the fact that *Cd19-cre* x flox-mHEL^{4X} Tg recipients expressed much lower overall concentrations of mHEL^{4X} in the spleen (Figure 6C). By contrast, Cre-dependent expression of mHEL^{4X} in liver hepatocytes (*Alb-cre*) (Postic et al., 1999) (Figure 6B) or the glomerular podocytes of the kidney (*NPHS2-cre*) (Moeller et al., 2003) and with no associated increase in splenic mHEL^{4X} expression (Figure 6C), did not affect either the accumulation of self-reactive Y53D⁺ B cells in the GC (Figure 6D) nor the production of anti-HEL^{4X} autoantibodies (Figure 6E).

Thus, although the specific expression of

foreign antigen and ultimately give rise to an autoantibody response (Figure S6).

GC Proximal Expression of Self-Antigen Is Required to Prevent Positive Selection of Self-Reactive GC B Cells

To examine the impact of the location of self-antigen expression on self-reactive GC B cells, we next utilized a series of Cre-transgenic mouse lines crossed with flox-mHEL^{4X} Tg mice to express high concentrations of mHEL^{4X} in a tissue and/or cell-type-specific manner (Figure S6). These mice again acted as recipients for SW_{HEL} B cells together with HEL^{3X}-SRBC foreign antigen. Specific expression of mHEL^{4X} on recipient B cells (*Cd19-cre*) (Rickert et al., 1997) (Figure 6A), which locate within and closely around GCs in the spleen, resulted in a virtual absence of Y53D⁺ SW_{HEL} B cell clones in splenic GCs (Figure 6D) and prevented the development of anti-HEL^{4X} serum antibody (Figure 6E).

relatively low amounts of self-antigen proximal to the GC micro-environment effectively prevented the positive selection of self-reactive GC B cells, this was not true of the same self-antigen expressed at high concentrations in distal organs. Localization of self-antigen proximal to the GC is therefore crucial to preventing positive selection and autoantibody-production by cross-reactive GC B cells (Figure S6).

Compensatory, Affinity-Reducing Mutations Permit Long-Term Survival of Y53D⁺ GC B Cells

Although self-antigen expressed proximal to the GC could effectively override positive selection of cross-reactive B cells generated in the GC, rare clones carrying apparently forbidden Y53D⁺ and Y53D⁺, Y58F⁺ self-reactive SW_{HEL} specificities were routinely found in GCs from mHEL^{4X} Tg and flox-mHEL^{4X} Tg mice challenged with HEL^{3X}-SRBC (Figure 5C). Although these could simply

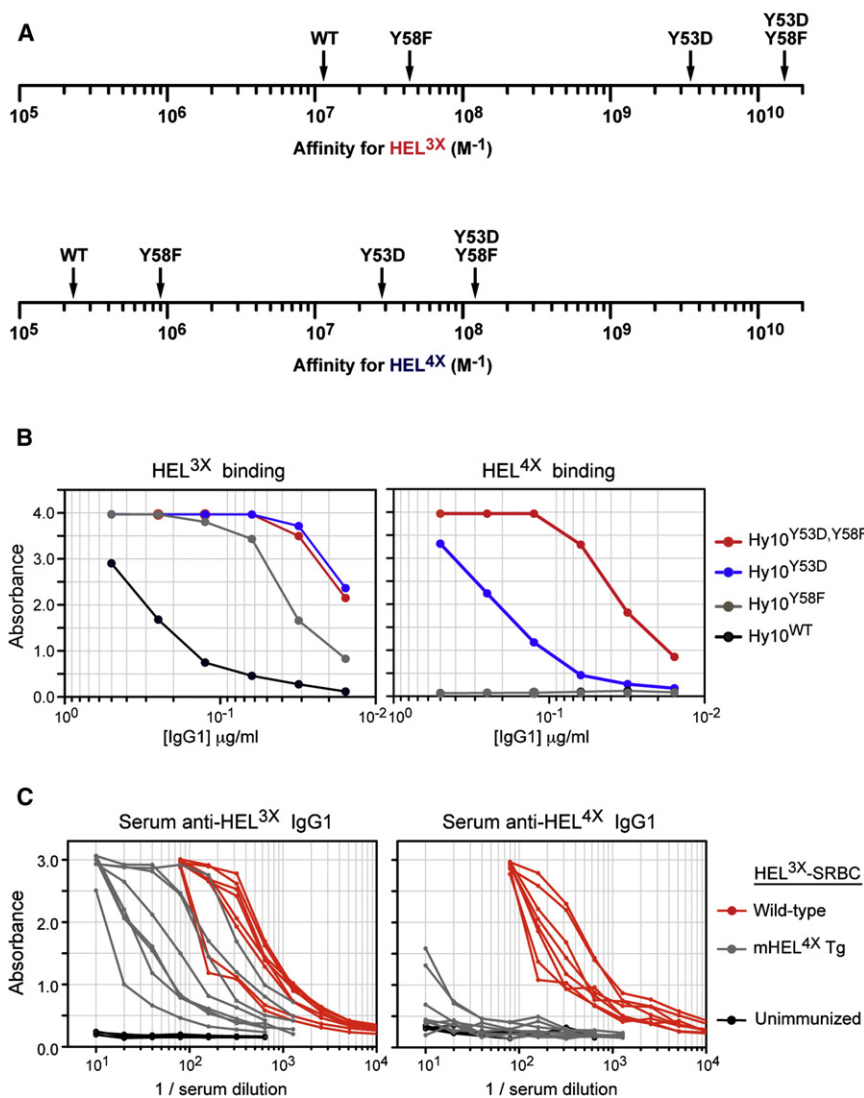


Figure 4. High-Affinity Autoantibodies Are Not Produced in mHEL^{4X} Tg Mice

(A) Distribution of affinities for HEL^{3X} and HEL^{4X} of WT HyHEL10 as well as specific HyHEL10 mutants carrying Y53D and/or Y58F substitutions (see Figure S4).

(B) ELISA of the binding of the indicated recombinant HyHEL10 molecules to HEL^{3X} and HEL^{4X}. Binding to HEL^{4X} is apparent in HyHEL10 carrying Y53D (with or without Y58F) but not Y58F alone.

(C) ELISA of HEL^{3X} and HEL^{4X} binding by serum IgG1 on day 21 of SW_{HEL} B cell responses to HEL^{3X}-SRBC. mHEL^{4X} Tg mice fail to produce anti-HEL^{4X} IgG1. Lines indicate titration data of sera from individual recipients, black lines representing data from unimmunized WT mice.

contain unusually high frequencies of substitutions in and around CDR1 and CDR3 coding regions of the Ig heavy-chain variable region, as well as in certain framework coding regions (Table S5). A group of specific mutations were present in Y53D⁺ GC B cell clones from mHEL^{4X} Tg, but not WT recipients (Tables S3 and S5), suggesting that these mutations may reduce rather than enhance the affinity of the SW_{HEL} BCR for HEL^{3X} and/or HEL^{4X}.

To test this proposition, we introduced these substitutions (L4F, I29S, S31N, S31Y, D32E, Y33F, Y58H, N94K; Table S5) into Y53D⁺ HyHEL10 IgG1 antibodies and their effect on HEL^{4X}-binding activity assessed by ELISA. In each case, the binding of Y53D⁺ HyHEL10 to HEL^{4X} was either greatly reduced or rendered undetectable (Figure S7A). These mutations were present in 76% of the Y53D⁺

represent transient self-reactive clones destined for removal from the GC, we sought to explore their significance in more detail. Reasoning that such cells may be expanded in the presence of stronger selection by foreign antigen, we analyzed the responses of SW_{HEL} B cells in WT, flox-mHEL^{4X} Tg and mHEL^{4X} Tg recipients challenged on day 0 with HEL^{3X}-SRBC foreign antigen as previously but also boosted with HEL^{3X}-SRBC 4 or 5 days later.

Boosting with HEL^{3X}-SRBC resulted in a 3- to 4-fold increase in the total number of SW_{HEL} GC B cells observed on day 21 of responses in recipients of all genotypes (data not shown). However, it failed to increase either the frequency of self-reactive (HEL^{4X}-binding) GC B cells (Figure 7A versus 5B) or the amount of anti-HEL^{4X} IgG1 (Figure 7B versus 5D) produced in recipients expressing either low (flox-mHEL^{4X} Tg) or high (mHEL^{4X} Tg) amounts of mHEL^{4X} self-antigen. Paradoxically, boosting mHEL^{4X} Tg recipients with HEL^{3X}-SRBC foreign antigen resulted in a 4-fold increase in the frequency of SW_{HEL} GC B cells carrying the Y53D substitution, such that they comprised ~40% of the population by day 21 of the response (Figure 7C versus 5C). On further analysis, the Y53D⁺ clones in mHEL^{4X} Tg recipients were found to

GC B cell clones sequenced from HEL^{3X}-SRBC boosted mHEL^{4X} Tg recipients (Figure 7D; Table S5). An additional 14% contained mutations predicted to reduce HEL^{4X}-binding by Y53D⁺ HyHEL10 based on their homology with verified inactivating mutations (N94H, N94R) or nonconservative substitution of a known HEL contact residue (T30I) (Figure 7D; Table S5). Importantly, all modified Y53D⁺ HyHEL10 molecules retained higher affinities for foreign antigen (HEL^{3X}) than the original HyHEL10 SW_{HEL} BCR (Figure S7B). Although we cannot exclude the possibility that mutations that were not analyzed here may impact on reactivity with HEL^{3X} and HEL^{4X}, our analysis does suggest that Y53D⁺ GC B cells in mHEL^{4X} Tg mice persist if they possess additional somatic mutation(s) that (1) decrease their affinity for self-antigen (HEL^{4X}) (Figure S7A) but (2) maintain increased affinity for foreign antigen (HEL^{3X}) (Figure S7B).

DISCUSSION

The threat to self-tolerance posed by SHM of the Ig variable region genes in GC B cells has been recognized since the

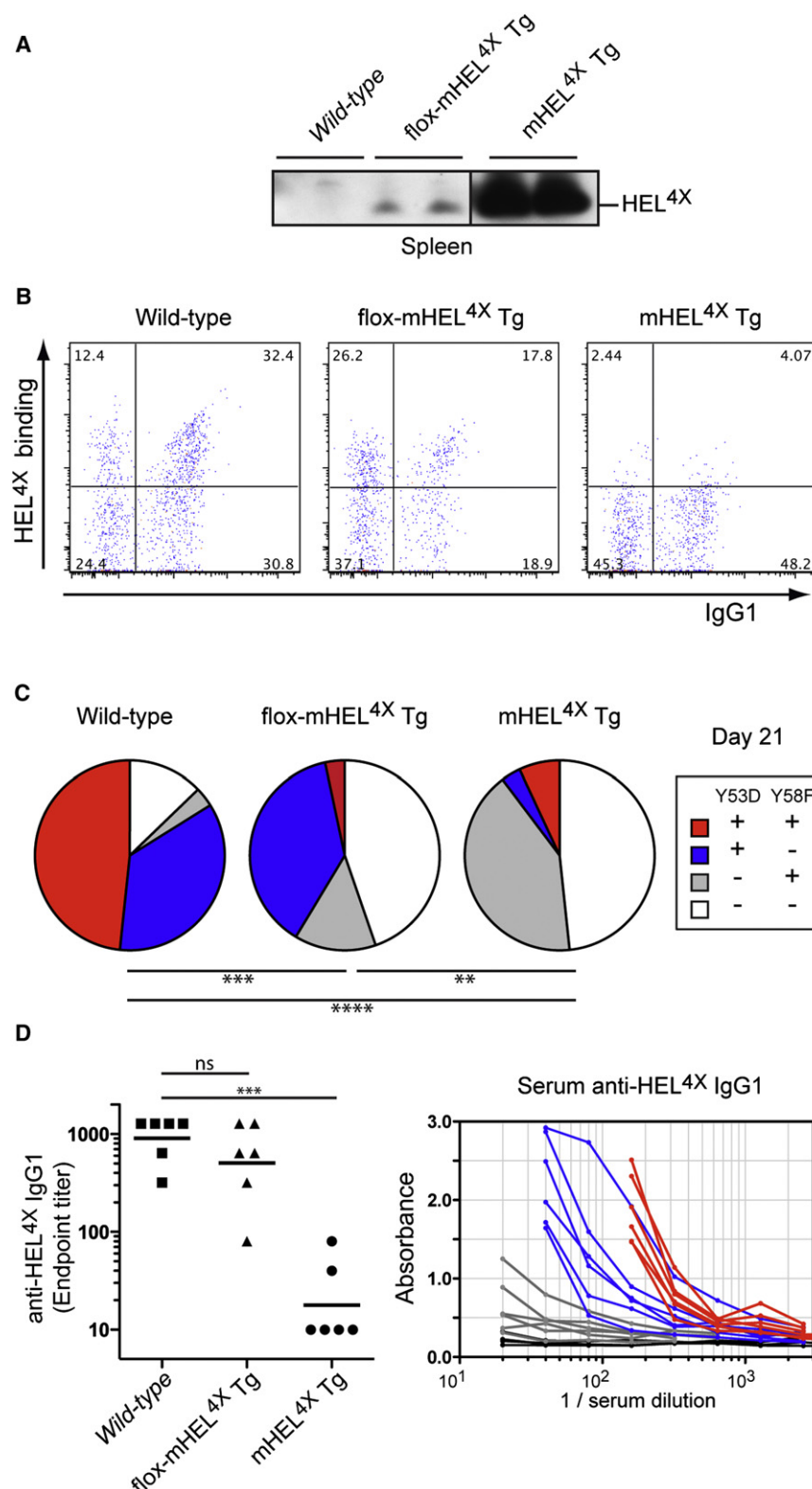


Figure 5. Self-Reactive GC B Cells Are Positively Selected and Produce Autoantibodies in flox-mHEL^{4X} Tg Mice

(A) Immunoprecipitation and protein immunoblot analysis of mHEL^{4X} expression in total spleen from the indicated mice. Low but detectable amounts of mHEL^{4X} were found in flox-mHEL^{4X} Tg mice. (B) Switching to IgG1 and HEL^{4X} binding capabilities of SW_{HEL} GC B cells on day 21 of responses to HEL^{3X}-SRBC. Self-reactive, HEL^{4X}-binding GC B cells were detected in flox-mHEL^{4X} but not mHEL^{4X} Tg mice. Plots are representative of 14 independent experiments (n = 3–6 per experimental group) and comprise concatenated data from three mice.

(C) Single cell SHM analysis of SW_{HEL} GC B cells on day 21. Clones analyzed: WT (n = 31 from 10 mice), flox-mHEL^{4X} Tg (n = 43 from ten mice), and mHEL^{4X} Tg (n = 38 from ten mice).

(D) Endpoint titer (left) and titration (right) analysis of anti-HEL^{4X} IgG1 in day 21 sera. Titration data is displayed as for Figure 4C, with data from the additional flox-mHEL^{4X} Tg recipient group shown in blue. Data is representative of seven independent experiments analyzed at day 21. ****p < 0.0001, ***p < 0.001, **p = 0.001 to 0.01; ns = not significant.

the dynamic and complex nature of SHM and selection within the GC has made it extremely difficult to identify and ascertain the fate of self-reactive B cells generated during this secondary phase of BCR diversification (Chan and Brink, 2012). The experimental model described here represents an important step forward in understanding how self-tolerance is enforced in the GC and how it may fail and give rise to autoimmunity. Thus, by challenging SW_{HEL} B cells with HEL^{3X} in the context of mHEL^{4X} self-antigen expression, we have developed the ability to (1) identify bona fide self-reactive B cells generated by SHM in the GC and (2) examine the fate of these cells when their target self-antigen is expressed at varying concentrations and in different locations.

Our major findings were that (1) self-reactive B cells can be effectively removed from the GC regardless of cross-reactivity with foreign antigen, (2) their removal depends on sufficient expression of the target self-antigen within or proximal to the GC, and (3) self-reactive GC B cells can escape deletion, undergo positive selection by

foreign antigen, and initiate an autoantibody response if target self-antigen expression is low or physically separate from the GC.

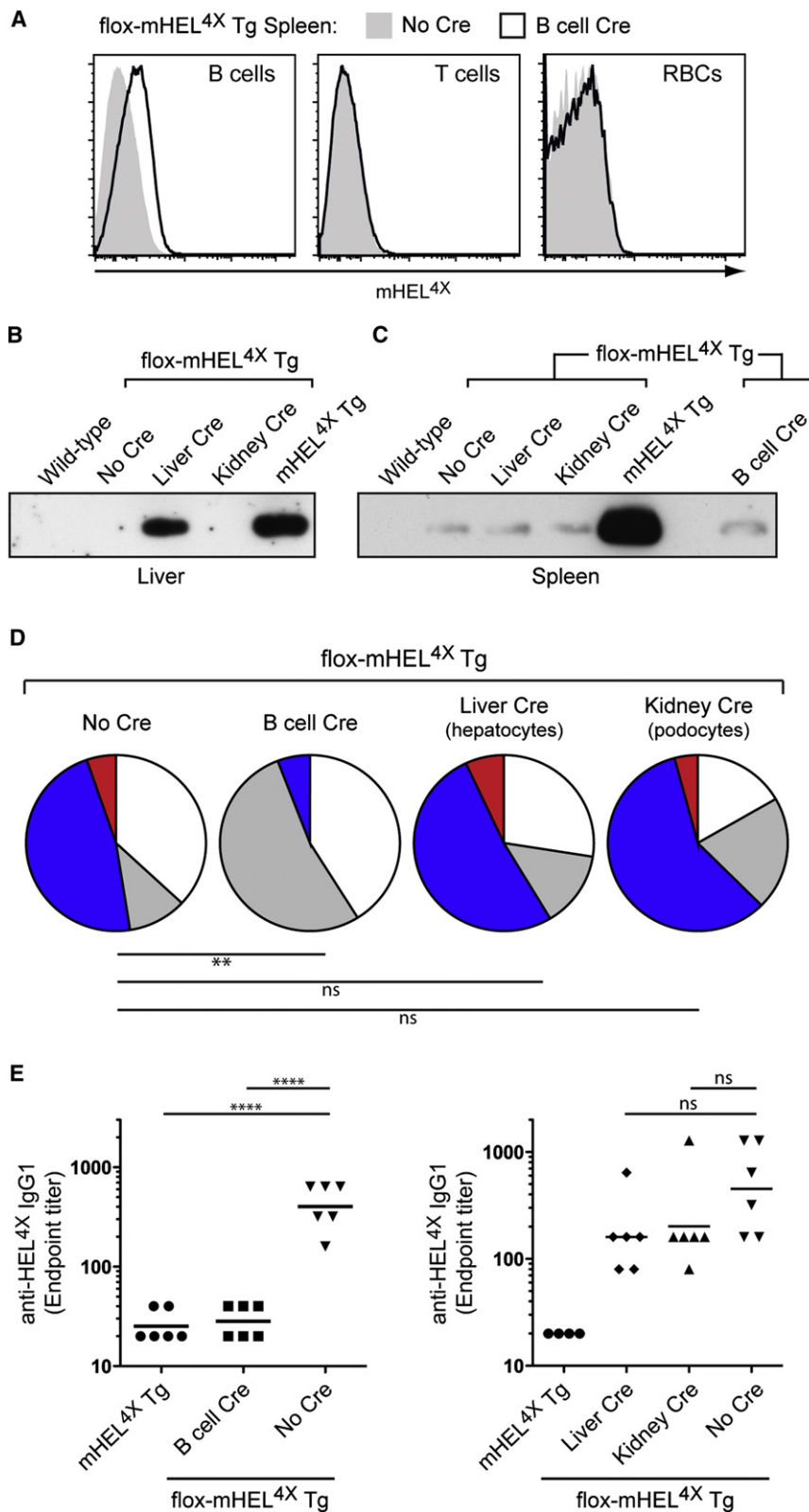


Figure 6. Failure of GC Self-Tolerance When Self-Antigen Is Expressed Distal to the GC

(A) Specific expression of mHEL^{4X} on splenic B cells from flox-mHEL^{4X} Tg mice carrying *Cd19-cre* transgene.

(B and C) Immunoprecipitation and protein immunoblot analysis of mHEL^{4X} expression in total liver or spleen from the indicated mice.

(D) Single cell SHM analysis of SW_{HEL} GC B cells on day 21 of SW_{HEL} B cell responses to HEL^{3X}-SRBC. Clones analyzed in flox-mHEL^{4X} Tg with: no Cre (n = 20), B cell Cre (n = 17), liver Cre (n = 29), kidney Cre (n = 24). SHM data comprise pooled data from two independent experiments (n = 6 per experimental group).

(E) Endpoint titer data of anti-HEL^{4X} IgG1 in day 21 sera. Data is representative of five independent experiments. ****p < 0.0001, **p = 0.001 to 0.01, ns = not significant.

against self-antigens expressed outside the GC microenvironment. Thus GC B cells that acquire reactivity with self-antigen expressed in a distal organ such as the liver remain susceptible to positive selection by cross-reactive foreign antigen and can therefore differentiate unimpeded into autoantibody-producing plasma cells. This failure to enforce self-tolerance to tissue-specific self-antigens in GC B cells stands in contrast to the purging of B and T lymphocytes recognizing this class of self-antigen at other checkpoints during lymphocyte differentiation. In the primary B cell repertoire, for instance, B cells recognizing tissue-specific antigens circulate through the body in a quiescent state and can be deleted or rendered inactive when they encounter their cognate self-antigen (Rojas et al., 2001; Russell et al., 1991). Furthermore, specialized medullary epithelial cells located in the thymus purge the early T cell repertoire of many clones reactive to distally expressed self-antigens by presenting peptides from these tissue-specific proteins (Mathis and Benoist, 2009). It is likely, therefore, that the incomplete control of self-reactive B cells generated in the GC represents a “weak link” in the mechanisms that collectively enforce self-tolerance in the immune system.

The failure to comprehensively enforce self-tolerance in the GC may be attributed

The most striking implication of these results is that there is no apparent mechanism in place to prevent self-reactive B cells generated in the GC from producing autoantibodies directed

to the difficulty of controlling self-reactive B cells generated in the midst of an active immune reaction against foreign antigen. Thus, in the absence of sufficient amounts of target self-antigen

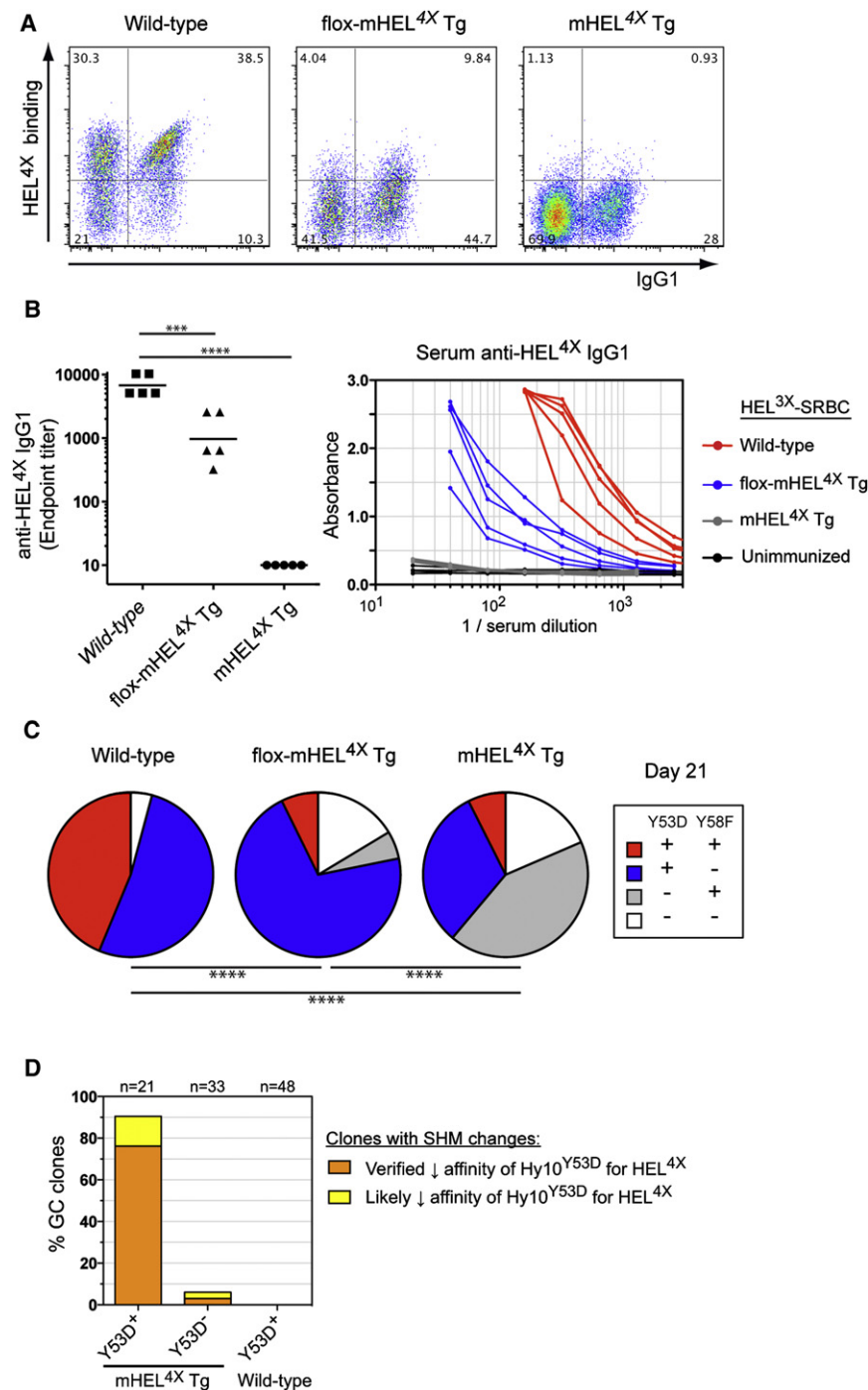


Figure 7. Boosting with Foreign Antigen Does Not Break GC B Cell Self-Tolerance

SW_{HEL} B cells were challenged and boosted with HEL^{3X}-SRBC. Data is from two independent experiments. Antigen boost was given on day 4 or day 5 without altering the response obtained.

(A) HEL^{4X} binding capabilities of SW_{HEL} GC B cells on day 21. Plots are representative of three independent experiments (n = 2–5 per experimental group) and comprise concatenated data from two mice.

(B) Endpoint titer (left) and titration (right) analysis of anti-HEL^{4X} IgG1 in sera from day 21 of responses. Titration data is displayed as for Figure 5D. ***p < 0.001, ****p < 0.0001.

(C) Single cell SHM analysis of SW_{HEL} GC B cells on day 21. The fraction of clones with Y53D is increased ~4-fold in mHEL^{4X} Tg mice given an antigen boost (compare with Figure 5C). Clones analyzed: WT (n = 48), flox-mHEL^{4X} Tg (n = 55), and mHEL^{4X} Tg (n = 54). SHM data comprise pooled data from six mice from two independent experiments. ***p < 0.001, ****p < 0.0001.

(D) Percentage of clones containing confirmed (orange) or likely (yellow) affinity-reducing mutations within the Y53D⁺ and Y53D⁻ GC B cell populations from mHEL^{4X} Tg recipient mice (Table S5) as well as the Y53D⁺ GC B cell population from WT recipient mice (Table S3). See Figure S7 for HEL^{4X} and HEL^{3X} binding analyses.

occurs during conventional immune responses is provided by the emergence of cross-reactive autoantibodies in response to viral antigens (Srinivasappa et al., 1986) and the frequent association of cross-reactive autoantibodies with postinfectious, tissue-specific autoimmune diseases such as hepatitis C-related immune thrombocytopenia (Zhang et al., 2009), pauci-immune focal necrotizing glomerulonephritis (Kain et al., 2008), Chagas disease (Cunha-Neto et al., 2006), Guillain-Barré syndrome (Yuki et al., 2004), and rheumatic carditis (Guilherme et al., 2006). Thus the inability of the immune system to prevent the production of cross-reactive autoantibodies from the GC response may contribute to the onset and/or progression of a number of human autoimmune diseases.

proximal to the GC microenvironment, self-reactive GC B cells remain “ignorant” of their self-reactivity and continue to receive help from GC-resident anti-foreign T_H cells. In this way, the production of antibodies against tissue-specific self-antigens can proceed without the need to compromise T cell self-tolerance. These findings imply that autoantibody production could emerge from any humoral immune response directed against a foreign antigen that has some structural homology to a tissue-specific self-antigen. Evidence that this phenomenon

One of the key implications of our findings is that the balance between the recognition of self and foreign antigens is critical to determining the fate of self-reactive GC B cells. In this regard, both the amount of each competing antigen type and the relative affinity of the BCR for them each play important roles. This point is illustrated by our finding that the reduced expression of mHEL^{4X} self-antigen in flox-mHEL^{4X} Tg versus mHEL^{4X} Tg mice permitted the positive selection of self-reactive Y53D⁺,Y58F⁻ GC B cells but still prevented the development

of the higher-affinity Y53D⁺,Y58F⁺ self-reactive clones. Mechanistically, we propose that the preferential association of GC B cells with self instead of foreign antigen prevents the reception of sufficient stimulatory signals from foreign antigen and limits their access to help from GC-resident T_{FH} cells (Victoria et al., 2010). Under such circumstances, self-reactive GC B cells would be at a competitive disadvantage compared to cells that recognize foreign but not self-antigen and so would fail to be propagated in the GC (eg Y53D⁺ versus Y53D⁻,Y58F⁺ clones in mHEL^{4X} Tg mice).

Another possibility is that the interaction of GC B cells with self versus foreign antigen leads to the delivery of quantitatively or qualitatively distinct signal(s) that result in the direct killing of self-reactive GC B cells. This may be true in particular when self-antigen is present at high concentrations, because GC B cells undergo rapid cell death when exposed to very high concentrations of exogenous antigen (Han et al., 1995; Pulentran et al., 1995; Shokat and Goodnow, 1995). In these models of GC negative selection, the death of antigen-reactive GC B cells was at least partially blocked by overexpression of the anti-apoptotic protein Bcl-2. Interestingly, this strategy reduces overall apoptosis in the GC and also blocks the death of GC B cells that would otherwise be removed due to their low affinity for foreign antigen (Smith et al., 2000). It will be of interest to determine whether the death of bona fide self-reactive B cells will also be blocked by overexpression of Bcl-2, or whether potentially other members of the Bcl-2 family, such as Mcl-1 (Vikstrom et al., 2010), may play a more prominent role.

Although the form of antigen used in this study provides a strong source of SRBC-specific T cell help to HEL^{3X}-binding SW_{HEL} B cells, it is possible that the use of alternative adjuvants and/or sources of T cell help might provide a stronger selection for foreign antigen and thus facilitate selection of cross-reactive GC B cells even when the target self-antigen is expressed at high concentrations. Separate experiments in which HEL^{3X} was conjugated to ovalbumin and injected in alum adjuvant failed to rescue self-reactive SW_{HEL} GC B cells or generate anti-HEL^{4X} autoantibodies in mHEL^{4X} Tg recipients (data not shown). This result, together with demonstration here that boosting with HEL^{3X}-SRBC also fails to break self-tolerance in mHEL^{4X} Tg mice, indicates that the enforcement of GC self-tolerance is robust when self-antigen is expressed at sufficient concentrations proximal to the GC. Nevertheless, it will be of interest to determine whether potentially stronger challenges, such as HEL^{3X} conjugated with TLR ligands or active pathogens, might more readily compromise GC self-tolerance and precipitate autoimmunity.

The results presented here reveal an exceptional capability for SHM-coupled positive and negative selection in the GC to shape BCR binding specificities to match the local antigen environment. While optimization of BCR affinity for foreign antigen drives the GC reaction, avoidance of cross-reactivity with localized self-antigen exerts a dominant influence that ultimately determines which somatic mutations can contribute to high affinity antibodies directed against foreign antigens. On the other hand, the failure of self-antigens expressed distal to the GC to have any impact on the secondary B cell repertoire represents an autoimmune risk. This “weak link” in self-tolerance is likely to contribute to the production of cross-reactive autoantibodies

that can recognize tissue-specific self-antigens and potentially to the genesis of postinfectious autoimmune disease.

EXPERIMENTAL PROCEDURES

HEL^{3X} and HEL^{4X} Proteins

HEL^{3X} is a recombinant version of HEL that carries the R21Q, R73E, and D101R substitutions (Paus et al., 2006). To produce HEL^{4X}, a pIRES expression plasmid was first produced carrying a cDNA encoding a membrane-bound form of HEL^{3X} (mHEL^{3X}) with the transmembrane and cytoplasmic domains of the H-2K^k class I major histocompatibility complex (MHC) molecule (Hartley et al., 1991). Candidate mHEL^{4X} molecules were produced by introducing a variety of amino acid substitutions at the K97 position and expressed separately on the surface of HEK293. The substitution chosen was K97R (Figure 1A). cDNAs encoding soluble, His-tagged versions of HEL^{3X} and HEL^{4X} were cloned into the pPIC9K vector and the recombinant proteins expressed in yeast (*Pichia pastoris*) and purified from culture supernatants (Paus et al., 2006).

flox-mHEL^{4X} Tg and mHEL^{4X} Tg Mice

An expression construct was assembled consisting of human ubiquitin C (*UBC*) promoter, *loxP*-flanked SV40 early polyadenylation site (pA), *FRT*-flanked mHEL^{3X} cDNA with 3' bovine growth hormone polyadenylation site, mHEL^{4X} cDNA with 3' bovine growth hormone polyadenylation site, murine phosphoglycerate kinase (*Pgk*) promoter, neomycin resistance gene (*neo*) cDNA, and a 3' splice donor sequence. A gene-targeting construct was assembled by inserting the expression construct between 5' and 3' homology arms from the murine *ROSA26* locus (Figure S2). Gene targeting in C57BL/6 Bruce4 embryonic stem cells was performed by Ozgene (Bentley, West Australia) and Tg founder mouse obtained carrying a single copy of the expression construct targeted to the *ROSA26* locus. This founder line (flox-mHEL^{3X} Tg) was crossed with *ACTB-FLPe* (Rodríguez et al., 2000) mice to obtain a germ-line deletion of the mHEL^{3X} cDNA and produce founders for the flox-mHEL^{4X} Tg line. flox-mHEL^{4X} Tg mice were in turn converted into founders for the mHEL^{4X} Tg line by crossing with a *ROSA26-cre* Tg line (Ozgene) to obtain germ-line deletion of the floxed polyadenylation site (Figure S2). Soluble HEL^{4X} is detectable in sera from mHEL^{4X} Tg mice (range 4–11 ng/ml in 6 mice) but is undetectable (<1 ng/ml) in straight flox-mHEL^{4X} Tg mice and all Cre Tg crosses.

Other Mice and SW_{HEL} B Cell Transfer Experiments

SW_{HEL} mice (Phan et al., 2003) were bred onto a CD45.1 congenic C57BL/6 background while all other mice were maintained on a pure C57BL/6 (CD45.2⁺) background. All mice were bred and housed in specific pathogen-free conditions at Australian Bioresources (Moss Vale, Australia) and the Garvan Institute. The following Cre Tg lines were used: *Cd19-cre* (Rickert et al., 1997), *Alb-cre* (Postic et al., 1999), *NPHS2-cre* (Moeller et al., 2003). Intravenous transfers of SW_{HEL} B cells (3 × 10⁴ HEL-binding B cells per recipient) together with HEL^{3X}-SRBC (2 × 10⁸ per recipient) were performed as described (Paus et al., 2006). All animal experiments were carried out in accordance with the guidelines of the Garvan St Vincent's Animal Ethics Committee.

Flow Cytometric Analysis

Staining procedures, reagents, data acquisition, and analysis of flow cytometry data have been previously described (Chan et al., 2009). Between 6–12 × 10⁵ events were collected per sample and light scatter gating performed to exclude dead cells and debris. A further doublet exclusion gate was applied and gates were set to exclude autofluorescent cells. GC B cells were identified within recipient spleen cell preparations as CD45.1⁺, CD45.2⁻, B220⁺, CD38^{lo} and typically comprised 0.1%–0.3% of total spleen cells. Binding of HEL^{3X} or HEL^{4X} by GC B cells was revealed by staining with the unlabelled proteins (50 ng/ml and 100 ng/ml, respectively) followed by HyHEL9-Alexa 647. Surface expression of mHEL^{4X} was detected directly with HyHEL9-Alexa647 and B cell, T cell, and red blood cell (RBC) subpopulations identified using the B220, CD3, and TER-119 lineage-specific markers, respectively.

Single-Cell Flow Cytometry Based Sorting and SHM Analysis

Cell suspensions were prepared as for flow cytometry analysis. Total donor-derived GC B cells were identified with anti-CD45.1-FITC, anti-CD38-PE, and anti-B220-APC. Single cell sorting was performed on a FACSaria (BD Biosciences) and the variable region exon of the SW_{HEL} Ig (HyHEL10) heavy chain gene amplified by PCR, sequenced and analyzed as previously described (Paus et al., 2006).

HEL^{3X} and HEL^{4X}-Binding ELISA

ELISA detection of the binding of recombinant HyHEL10 IgG1 molecules and serum antibodies to HEL^{3X} and HEL^{4X} were performed as previously described (Phan et al., 2003) except HEL^{3X} or HEL^{4X} protein coated 384-well plates (Corning) were used. To quantify serum antibody concentrations, endpoint titers were calculated based on 97.5% confidence levels or greater (Frey et al., 1998).

Immunofluorescence Histology

Sections were cut and prepared as previously described (Chan et al., 2009). Detection of mHEL^{4X} expression was with polyclonal rabbit anti-HEL IgG (Rockland Immunochemicals) followed by Alexa 555-conjugated anti-rabbit IgG(H+L) (Invitrogen Molecular Probes). Naive B cells were revealed with anti-IgD-Alexa 647 (clone 11-26c.2a, BD Biosciences) and GCs using PNA-FITC (Vector Laboratories).

Detection of HEL^{4X} Expression by Immunoprecipitation and Protein Immunoblots

Equivalent tissue amounts by weight were homogenized in RIPA buffer and immunoprecipitated at 4°C using Protein G beads and purified HyHEL9 monoclonal antibody. Immunoblotting was performed as previously described (Gardam et al., 2008) with membranes probed with polyclonal rabbit anti-HEL IgG (Rockland) followed by sheep anti-rabbit IgG-HRP (Santa Cruz).

Recombinant HyHEL10 IgG1 Antibody Production and Binding Affinity Analysis

WT and mutant recombinant HyHEL10 IgG1 mAbs were expressed in CHO cells as previously described (Phan et al., 2006). Biacore analysis was performed at 25°C using a Biacore 2000 (GE Healthcare). Anti-mouse IgG1 monoclonal antibody (A85-1, BD Biosciences) was immobilized onto a CM5 sensor chip (GE Healthcare) using amine coupling to attain a target density of 10,000 RU. HyHEL10 IgG1 mutants were then injected to achieve a reading of 1,000 RU. Binding of antigen was assessed by injecting serial dilutions of HEL^{3X} or HEL^{4X} (5.6 μM–1.0 nM) over all flow cells at a flow rate of 30 μl/min until equilibrium was reached. Equilibrium binding constants (K_d) were determined by fitting sensorgrams to a 1:1 Langmuir binding model using BIAevaluation 4.1 program (GE Healthcare). Where association and dissociation rates could not be determined using kinetic fits, binding affinity was determined by Scatchard plot analysis using responses obtained during steady-state phase of binding.

Statistical Analysis

Statistical significance of serum antibody endpoint titers and SHM data were calculated using Graphpad Prism software. For endpoint titers, multiple comparisons were performed using ANOVA analyses with the Bonferroni post-test and 99.9% confidence levels applied. Statistical analyses of the SHM data were performed using the chi-square test and 99% confidence intervals applied.

SUPPLEMENTAL INFORMATION

Supplemental Information includes seven figures and five tables and can be found with this article online at <http://dx.doi.org/10.1016/j.immuni.2012.07.017>.

ACKNOWLEDGMENTS

This work was funded by the National Health and Medical Research Council of Australia (Program Grant 427620). We thank L. Holzman (University of Michigan) for supplying *NPHS2-cre* Tg mice. We also thank T. Phan, N. Krautler,

S. Tangye, and C. Goodnow for helpful discussions and advice; C. Brownlee and N. Alling for single cell FACS sorting; D. Christ, R. Rouet, and P. Schofield for assistance with Biacore analysis; and the staff of Australian Bioresources (Moss Vale) and the Garvan Institute animal facilities. We also thank Ozgene (Bentley, West Australia) for production of mHEL^{4X} Tg mice.

Received: April 28, 2012

Accepted: July 12, 2012

Published online: November 8, 2012

REFERENCES

- Ait-Azzouzene, D., Kono, D.H., Gonzalez-Quintial, R., McHeyzer-Williams, L.J., Lim, M., Wickramarachchi, D., Gerdes, T., Gavin, A.L., Skog, P., McHeyzer-Williams, M.G., et al. (2010). Deletion of IgG-switched autoreactive B cells and defects in Fas(lpr) lupus mice. *J. Immunol.* 185, 1015–1027.
- Allen, C.D., and Cyster, J.G. (2008). Follicular dendritic cell networks of primary follicles and germinal centers: phenotype and function. *Semin. Immunol.* 20, 14–25.
- Casson, L.P., and Manser, T. (1995). Random mutagenesis of two complementarity determining region amino acids yields an unexpectedly high frequency of antibodies with increased affinity for both cognate antigen and autoantigen. *J. Exp. Med.* 182, 743–750.
- Chan, T.D., and Brink, R. (2012). Affinity-based selection and the germinal center response. *Immunol. Rev.* 247, 11–23.
- Chan, T.D., Gatto, D., Wood, K., Camidge, T., Basten, A., and Brink, R. (2009). Antigen affinity controls rapid T-dependent antibody production by driving the expansion rather than the differentiation or extrafollicular migration of early plasmablasts. *J. Immunol.* 183, 3139–3149.
- Cunha-Neto, E., Bilate, A.M., Hyland, K.V., Fonseca, S.G., Kalil, J., and Engman, D.M. (2006). Induction of cardiac autoimmunity in Chagas heart disease: a case for molecular mimicry. *Autoimmunity* 39, 41–54.
- Diamond, B., and Scharff, M.D. (1984). Somatic mutation of the T15 heavy chain gives rise to an antibody with autoantibody specificity. *Proc. Natl. Acad. Sci. USA* 81, 5841–5844.
- Frey, A., Di Canzio, J., and Zurakowski, D. (1998). A statistically defined endpoint titer determination method for immunoassays. *J. Immunol. Methods* 221, 35–41.
- Gardam, S., Sierro, F., Basten, A., Mackay, F., and Brink, R. (2008). TRAF2 and TRAF3 signal adapters act cooperatively to control the maturation and survival signals delivered to B cells by the BAFF receptor. *Immunity* 28, 391–401.
- Goodnow, C.C. (1992). Transgenic mice and analysis of B-cell tolerance. *Annu. Rev. Immunol.* 10, 489–518.
- Goodnow, C.C., Vinuesa, C.G., Randall, K.L., Mackay, F., and Brink, R. (2010). Control systems and decision making for antibody production. *Nat. Immunol.* 11, 681–688.
- Guay, H.M., Panarey, L., Reed, A.J., and Caton, A.J. (2004). Specificity-based negative selection of autoreactive B cells during memory formation. *J. Immunol.* 173, 5485–5494.
- Guilherme, L., Kalil, J., and Cunningham, M. (2006). Molecular mimicry in the autoimmune pathogenesis of rheumatic heart disease. *Autoimmunity* 39, 31–39.
- Han, S., Zheng, B., Dal Porto, J., and Kelsoe, G. (1995). In situ studies of the primary immune response to (4-hydroxy-3-nitrophenyl)acetyl. IV. Affinity-dependent, antigen-driven B cell apoptosis in germinal centers as a mechanism for maintaining self-tolerance. *J. Exp. Med.* 182, 1635–1644.
- Hartley, S.B., Crosbie, J., Brink, R., Kantor, A.B., Basten, A., and Goodnow, C.C. (1991). Elimination from peripheral lymphoid tissues of self-reactive B lymphocytes recognizing membrane-bound antigens. *Nature* 353, 765–769.
- Kain, R., Exner, M., Brandes, R., Ziebmayer, R., Cunningham, D., Alderson, C.A., Davidovits, A., Raab, I., Jahn, R., Ashour, O., et al. (2008). Molecular mimicry in pauci-immune focal necrotizing glomerulonephritis. *Nat. Med.* 14, 1088–1096.

- King, C., Tangye, S.G., and Mackay, C.R. (2008). T follicular helper (TFH) cells in normal and dysregulated immune responses. *Annu. Rev. Immunol.* 26, 741–766.
- MacLennan, I.C. (1994). Germinal centers. *Annu. Rev. Immunol.* 12, 117–139.
- MacLennan, I.C., Toellner, K.M., Cunningham, A.F., Serre, K., Sze, D.M., Zúñiga, E., Cook, M.C., and Vinuesa, C.G. (2003). Extrafollicular antibody responses. *Immunol. Rev.* 194, 8–18.
- Mathis, D., and Benoist, C. (2009). Aire. *Annu. Rev. Immunol.* 27, 287–312.
- Moeller, M.J., Sanden, S.K., Soofi, A., Wiggins, R.C., and Holzman, L.B. (2003). Podocyte-specific expression of cre recombinase in transgenic mice. *Genesis* 35, 39–42.
- Nemazee, D. (1993). Promotion and prevention of autoimmunity by B lymphocytes. *Curr. Opin. Immunol.* 5, 866–872.
- Nossal, G.J. (1988). Somatic mutations in B lymphocytes: new perspectives in tolerance research? *Immunol. Cell Biol.* 66, 105–110.
- Nossal, G.J. (1994). Negative selection of lymphocytes. *Cell* 76, 229–239.
- Notidis, E., Heltemes, L., and Manser, T. (2002). Dominant, hierarchical induction of peripheral tolerance during foreign antigen-driven B cell development. *Immunity* 17, 317–327.
- Olee, T., Lu, E.W., Huang, D.F., Soto-Gil, R.W., Deftos, M., Kozin, F., Carson, D.A., and Chen, P.P. (1992). Genetic analysis of self-associating immunoglobulin G rheumatoid factors from two rheumatoid synovia implicates an antigen-driven response. *J. Exp. Med.* 175, 831–842.
- Padlan, E.A., Silverton, E.W., Sheriff, S., Cohen, G.H., Smith-Gill, S.J., and Davies, D.R. (1989). Structure of an antibody-antigen complex: crystal structure of the HyHEL-10 Fab-lysozyme complex. *Proc. Natl. Acad. Sci. USA* 86, 5938–5942.
- Paus, D., Phan, T.G., Chan, T.D., Gardam, S., Basten, A., and Brink, R. (2006). Antigen recognition strength regulates the choice between extrafollicular plasma cell and germinal center B cell differentiation. *J. Exp. Med.* 203, 1081–1091.
- Phan, T.G., Amesbury, M., Gardam, S., Crosbie, J., Hasbold, J., Hodgkin, P.D., Basten, A., and Brink, R. (2003). B cell receptor-independent stimuli trigger immunoglobulin (Ig) class switch recombination and production of IgG autoantibodies by anergic self-reactive B cells. *J. Exp. Med.* 197, 845–860.
- Phan, T.G., Gardam, S., Basten, A., and Brink, R. (2005). Altered migration, recruitment, and somatic hypermutation in the early response of marginal zone B cells to T cell-dependent antigen. *J. Immunol.* 174, 4567–4578.
- Phan, T.G., Paus, D., Chan, T.D., Turner, M.L., Nutt, S.L., Basten, A., and Brink, R. (2006). High affinity germinal center B cells are actively selected into the plasma cell compartment. *J. Exp. Med.* 203, 2419–2424.
- Plotkin, S.A., Orenstein, W.A., and Offit, P.A. (2008). *Vaccines*, Fifth Edition (Philadelphia, USA: Elsevier).
- Postic, C., Shiota, M., Niswender, K.D., Jetton, T.L., Chen, Y., Moates, J.M., Shelton, K.D., Lindner, J., Cherrington, A.D., and Magnuson, M.A. (1999). Dual roles for glucokinase in glucose homeostasis as determined by liver and pancreatic beta cell-specific gene knock-outs using Cre recombinase. *J. Biol. Chem.* 274, 305–315.
- Pulendran, B., Kannourakis, G., Nouri, S., Smith, K.G., and Nossal, G.J. (1995). Soluble antigen can cause enhanced apoptosis of germinal-centre B cells. *Nature* 375, 331–334.
- Rickert, R.C., Roes, J., and Rajewsky, K. (1997). B lymphocyte-specific, Cre-mediated mutagenesis in mice. *Nucleic Acids Res.* 25, 1317–1318.
- Rodríguez, C.I., Buchholz, F., Galloway, J., Sequerra, R., Kasper, J., Ayala, R., Stewart, A.F., and Dymecki, S.M. (2000). High-efficiency deleter mice show that FLPe is an alternative to Cre-loxP. *Nat. Genet.* 25, 139–140.
- Rojas, M., Hulbert, C., and Thomas, J.W. (2001). Anergy and not clonal ignorance determines the fate of B cells that recognize a physiological autoantigen. *J. Immunol.* 166, 3194–3200.
- Russell, D.M., Dembić, Z., Morahan, G., Miller, J.F., Bürki, K., and Nemazee, D. (1991). Peripheral deletion of self-reactive B cells. *Nature* 354, 308–311.
- Shlomchik, M.J., Marshak-Rothstein, A., Wolfowicz, C.B., Rothstein, T.L., and Weigert, M.G. (1987). The role of clonal selection and somatic mutation in autoimmunity. *Nature* 328, 805–811.
- Shlomchik, M., Mascal, M., Shan, H., Radic, M.Z., Pisetsky, D., Marshak-Rothstein, A., and Weigert, M. (1990). Anti-DNA antibodies from autoimmune mice arise by clonal expansion and somatic mutation. *J. Exp. Med.* 171, 265–292.
- Shokat, K.M., and Goodnow, C.C. (1995). Antigen-induced B-cell death and elimination during germinal-centre immune responses. *Nature* 375, 334–338.
- Smith, K.G., Light, A., O'Reilly, L.A., Ang, S.M., Strasser, A., and Tarlinton, D. (2000). bcl-2 transgene expression inhibits apoptosis in the germinal center and reveals differences in the selection of memory B cells and bone marrow antibody-forming cells. *J. Exp. Med.* 191, 475–484.
- Srinivasappa, J., Saegusa, J., Prabhakar, B.S., Gentry, M.K., Buchmeier, M.J., Wiktor, T.J., Koprowski, H., Oldstone, M.B., and Notkins, A.L. (1986). Molecular mimicry: frequency of reactivity of monoclonal antiviral antibodies with normal tissues. *J. Virol.* 57, 397–401.
- Tarlinton, D.M. (2008). Evolution in miniature: selection, survival and distribution of antigen reactive cells in the germinal centre. *Immunol. Cell Biol.* 86, 133–138.
- Tiller, T., Tsuiji, M., Yurasov, S., Velinzon, K., Nussenzweig, M.C., and Wardemann, H. (2007). Autoreactivity in human IgG+ memory B cells. *Immunity* 26, 205–213.
- Victoria, G.D., Schwickert, T.A., Fooksman, D.R., Kamphorst, A.O., Meyer-Hermann, M., Dustin, M.L., and Nussenzweig, M.C. (2010). Germinal center dynamics revealed by multiphoton microscopy with a photoactivatable fluorescent reporter. *Cell* 143, 592–605.
- Vikstrom, I., Carotta, S., Lüthje, K., Peperzak, V., Jost, P.J., Glaser, S., Busslinger, M., Bouillet, P., Strasser, A., Nutt, S.L., and Tarlinton, D.M. (2010). Mcl-1 is essential for germinal center formation and B cell memory. *Science* 330, 1095–1099.
- Wardemann, H., Yurasov, S., Schaefer, A., Young, J.W., Meffre, E., and Nussenzweig, M.C. (2003). Predominant autoantibody production by early human B cell precursors. *Science* 301, 1374–1377.
- Yuki, N., Susuki, K., Koga, M., Nishimoto, Y., Odaka, M., Hirata, K., Taguchi, K., Miyatake, T., Furukawa, K., Kobata, T., and Yamada, M. (2004). Carbohydrate mimicry between human ganglioside GM1 and *Campylobacter jejuni* lipooligosaccharide causes Guillain-Barre syndrome. *Proc. Natl. Acad. Sci. USA* 101, 11404–11409.
- Zhang, W., Nardi, M.A., Borkowsky, W., Li, Z., and Karpatsky, S. (2009). Role of molecular mimicry of hepatitis C virus protein with platelet GPIIb in hepatitis C-related immunologic thrombocytopenia. *Blood* 113, 4086–4093.